

Assessment of Total Harmonics Effects on Grid-Connected Powered Inverter Using Sine-Referenced and Static-band Hysteresis of Current Controllers

CANDIDUS.U EYA¹, OMEJE CRESCENT.O², NWOKOCHA NATHAN³, BENJAMIN N.UGWU⁴

¹Electrical Engineering, University of Nigeria Nsukka, NIGERIA

¹Africa Centre of Excellence, University of Nigeria, NIGERIA

²Electrical and Electronics, University of Port Harcourt, Rivers State, NIGERIA

³Federal College of Education (Tech), Omoku, Rivers State, NIGERIA

⁴Electrical/Electronics Engineering, Enugu State Polytechnic, Iwollo, NIGERIA

Abstract—This article presents an assessment of total harmonics effects on grid-connected powered inverter using sine-referenced and static-band hysteresis of current controllers. To realize this art, current transducer, static-band and sine-referenced hysteresis current controllers, solar energy source, maximum power point tracker, grid supply and voltage source DC-AC converter are engaged. The system has these features are: (i) Light weight owing to none transformer-less system application (ii) Efficient in injection of power

Under static-band hysteresis current controlled fed-back system, at upper and lower bands of 130V and 50V, a total harmonic distortion, THD of 1.815% and output voltage, v_o of 220Vrms (320V peak) were realized whereas in sine-referenced band hysteresis current controlled fed-back system at upper and lower bands of 430V and 340V, a THD of 1.019% and v_o of 220Vrms are released. The computer simulations and spectral analyses of the system were presented

Keywords— : Assessment, DC-AC Converter, Static-band, Grid-connected, sine-referenced, Hysteresis.

Received: May 18, 2021. Revised: February 21, 2022. Accepted: March 20, 2022. Published: April 27, 2022.

1. Introduction

Harmonics is the increasing frequency waveform, overlaid upon the fundamental frequency that is adequate to deface its wave-shape. Harmonics rises in power electronic systems as a result of introduction of power electronics drives for alternating current-to-direct current motors, direct current fans, pumps, etc [1].

The consequences of excessive presence of harmonics in power electronics systems-based devices such as in grid-connected inverter systems, are flopping of some load needs, hotness in the system, superfluous voltage, blunder in metering and control, faulty of relays operations, fading in communication and control signals [2]. There are innumerable means of mitigating total harmonics distortions (THD) in power electronic systems. A few of them are: waveform regulation by transformer connections, pulse-width modulation schemes, waveform control by multiple commutations in each cycle, waveform controlled by using delta-star transformer output, utilization of filters, and high pulsed rectifier cascading. In PWM, there are various sub-divisions such as carrier-based modulation schemes, third harmonic-injection method, space vector modulation, and random pulse width

modulation with their merits and demerits. Example, in random pulse width modulation scheme, it relies majorly on randomizing the frequency of the carrier waveform in order to allocate the intense energy of the harmonic frequency of the DC-AC converter output voltage in a constricted high frequency range. The vital advantage of this scheme is to mitigate the energy of the harmonics, which in turn will minimize the THD of the DC-AC converter output voltage [3-10]. But, this act definitely will also distress the energy of the basic frequency component by reducing the size of the amplitude that affects the value of waveform.

The main purpose of this paper is to investigate the percentage level of total harmonics distortion on single phase grid-connected powered inverter using sinusoidal and fixed-band hysteresis of current controllers. A key and distinguishing feature of the power circuit configuration in this research work is that in case of any short-circuit condition between the power MOSFETS on the same leg, the system can handle it without any device blow due to the presence of inductors L_a and L_b as shown in Fig.1 unlike in conventional H-bridge inverter systems[11-17].

2. Methodology

The major component values used in this paper are listed in Table 1. The circuit diagram is shown in Fig.1. The method that is adopted in this research is all about analytical and simulation methods.

Table1. Materials used in this work

Components	Values
PV module Voltage	72V
Grid Frequency	50Hz
Grid Voltage	220V
Duty ratio	0.850
L and Lo inductors	1.15mH and 9.5mH
Input Capacitor & R6030ENXC7G MOSFET	1000uF & 600V
Carrier frequency	23kHz

3. Principle Operation of the Grid-connected DC-AC Converter System

Once the peak power is sensed, the signal is communicated to the analog-to-digital converter, (A/DC) in control section. The A/DC digitizes signal and delivers it to the controller's signal processing section. The control section then triggers DC-DC boost converter into operation. Under this condition, the output voltage of the combined solar panels is raised appreciably which is delivered to inverter input terminals after matching the voltage per current of PV and the boost converter voltage per current. The DC-AC converter remains in idle mode as long as no firing signals are placed on the gate terminals of the switches. However, once triggering pulses (vg21 and vg22) strike the gate terminals of the MOSFETS (MS1, MS2), it establishes a gate to source voltage more than or equal to the edge voltage to open up the channel of the MOSFET. Therefore, the previously developed voltage between drain and the source, pumps the greater carriers from the source to drain terminals through the inversion layers, which transform the DC power TO AC power. The complementary triggering pulses (vg23 and vg24) turn on MOSFETS (MS3, MS4) during the negative half-cycled operation. The output waveform of the DC-AC converter is a square form-based waveform. Then an inductor, Lo filters the ripples and removes most of the harmonics to generate a triangular-sinusoidal waveform as the inductor output waveform. The controller section has a defined region, which contains the referenced current, the top current band bound and lesser band bound.

The output filter inductor in Fig.1 also acts as a harmonizing point between the DC-AC converter and the grid supply. As soon as the output of the inductor is made, the regulator section forces it to trail the modulating current in-between the top and low band bounds respectively in order to be injected to the utility network at power factor of either the sine-referenced band or static-band current controller applied

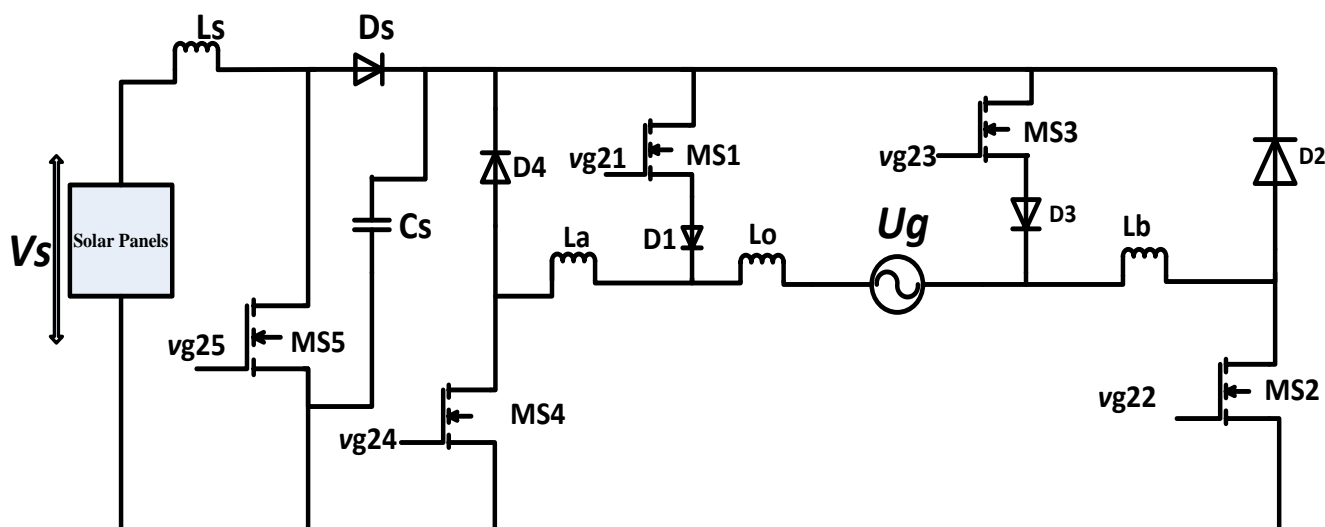


Fig.1. Proposed Power Circuit of the system drawn in proteus

The instantaneous voltage across the DC-AC converter output can be written as follow:

$$V_{inv} = V_L + V_{grid} \quad (1)$$

$$v_{inv} = \frac{L di_L(t)}{dt} + V_m \cos(\omega t - \pi/2) \quad (2)$$

$$i_L(t) = \frac{1}{L} \int_0^T (v_{inv} - V_m \cos(\omega t - \pi/2)) \quad (3)$$

V_{inv} - Instantaneous DC/AC voltage, L - inductance of output inductor, V_m - peak utility voltage, ω - circular frequency, i_L - instantaneous current of the output inductor and T - operating period.

4. Harmonization of Filtered DC-AC Converter Current and Voltage of the Grid

When the prime current is recognized in the proposed system, the DC-AC converter delivers it to the power grid via the action of switching ON and OFF of the power MOSFET switches. The control side of the AC part comprises comparator, the current band regulator, reference sine wave storage part, signal storage entity, A/D converter and sensory current device. The sensory current device detects the current passing through the inductor and delivers the signal to the comparator. This hysteresis comparator compares the inductor current with the top(upper) and lower current band bounds due to the operations of hysteresis current controller schemes that could either be static-band current controller or sine-referenced current controller to get the gratification of IEEE Std 929-2000 for suitable delivering of DC power into grid. Those two schemes were applied in this research work. And their analyses are deduced as follow:

5. Synchronization of Inverter Current and Grid Voltage by Static-band Current Controller

The procedure of the static-band current regulator is expressed in eq.4:

If the alternating current from the utility supply current at $n=1$ and is written as:

$$i_{ref} = I_m \cos(\omega t - \pi/2) \quad (4)$$

For the top current band, i_u is expressed as

$$i_u = i_{ref} + H \quad (5)$$

Then, the lower current limit, i_l of the wave shape is expressed as in eq.6

$$i_l = i_{ref} - H \quad (6)$$

If $i_L > i_{up}$; switch OFF MS1 and MS2; turn ON S3 and S4;

$v_{inv} = -V_{mpp}$ but If $i_L < i_L$; Turn OFF S3 and S4 ;turn ON MS1 and MS2; I_{max} = peak of the modulating current, i_L - output inductor current, H - band limit of the hysteresis ; i_{up} - top band current;

i_L - lower band current; i_{ref} - reference current

If the inductor current flowing is sensed by the current sensing device, it delivers the message to the comparator for judgement. When the inductor current is more than upper current band level, the comparator outputs the error current signal to trigger the power switches by switching OFF MS1 and MS2; and holding ON MS3 and MS4 in order to decrease the current gradient and to force the inductor to trail the modulating current. In addition to that, the output voltage of the DC/AC converter will be very close to the boosted peak DC voltage with negative signal. However if the filtered DC/AC converter current is smaller than the lower current band bound, the comparator establishes current error signal that switches OFF MS3 and MS4; and switches ON MS1 and MS2 for raising the current gradient so that the inductor current is limited within the hysteresis band bounds. Under this prevailing situation the output voltage across the DC/AC converter is at the peak. Therefore the continuously dwindling and raising up of current gradient as the inductor current is passing ensures suitable harmonization of the filtered DC/AC converter current to bear the equal frequency and in phase with the grid voltage. Henceforth, it brings the power factor of the system at unity. Fig.2 illustrated simulated result of the static-band hysteresis current based regulator used for regulating the DC-AC current injection in to the grid network.

Furthermore, the harmonization of DC-AC current and utility voltage at unity power factor wave shapes is displayed Fig.4. But provided the output inductor current is contained within the band, the regulator continues on its usual switching state. And once it tracks it well, the current passing through inductor and the grid voltage concurrently start from the similar origin, rise at their peak points of various amplitudes at angles of $\pi/2$ and π , returns to origin at angles π and 2π to complete one cycle. Under this situation, they are described to be harmonized and at power factor of 1 (unity).

The Fig.2 shows static-band current controller waveforms. They are generated by the equations 4, 5 and 6 and are applied in control unit in Simpler software used in controlling utility-connected DC-AC voltage system of Fig.1. The upper band limit, lower limit and peak reference voltage are 130V, 50V and 90V. The current tracker explore between these two bands to ensure good synchronization (harmonization) between the DC-AC converter output current and the utility voltage

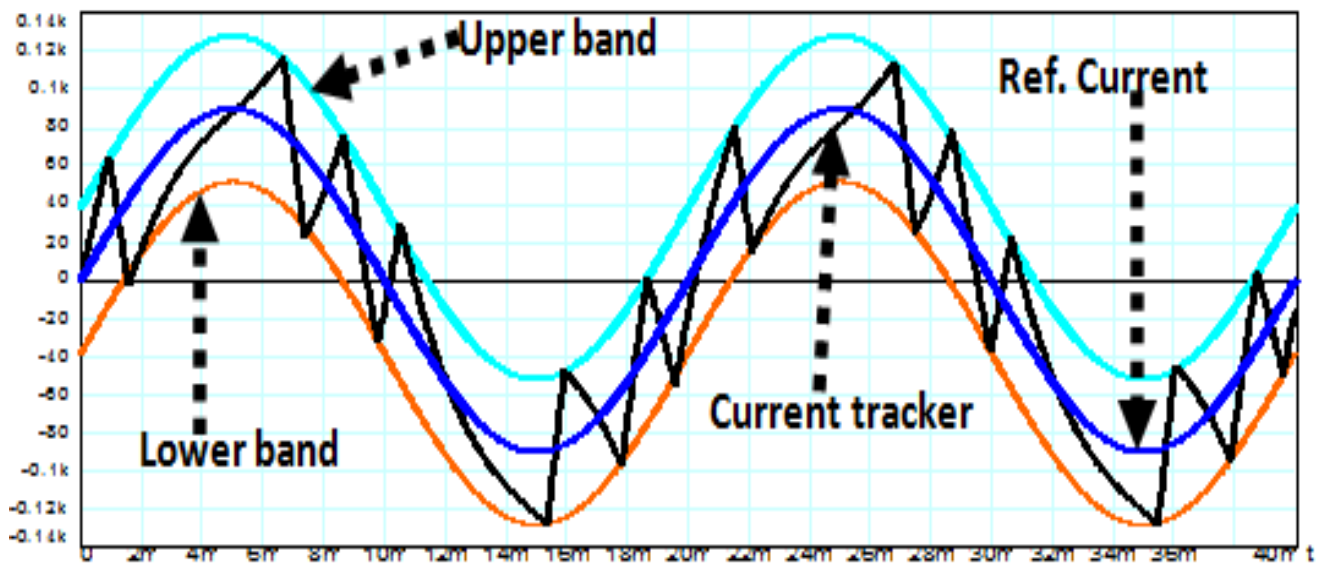


Fig.2: Static-band current regulator wave shapes

The Fig.3 showed that the peak synchronized voltage is 320.00V and peak harmonized current of 98.00A was injected into grid system. The current distortion was reduced, however not wiped because of presence of asymmetrical frequencies

accompanied with the static-band hysteresis based-current regulator on the course of controlling the passage of current to the grid system. The harmonic spectral order of the output inductor current was done with Fast Fourier Transform (FFT) and is displayed in Fig.4. The spectral value of total harmonic distortion (THD) is 1.8146%.

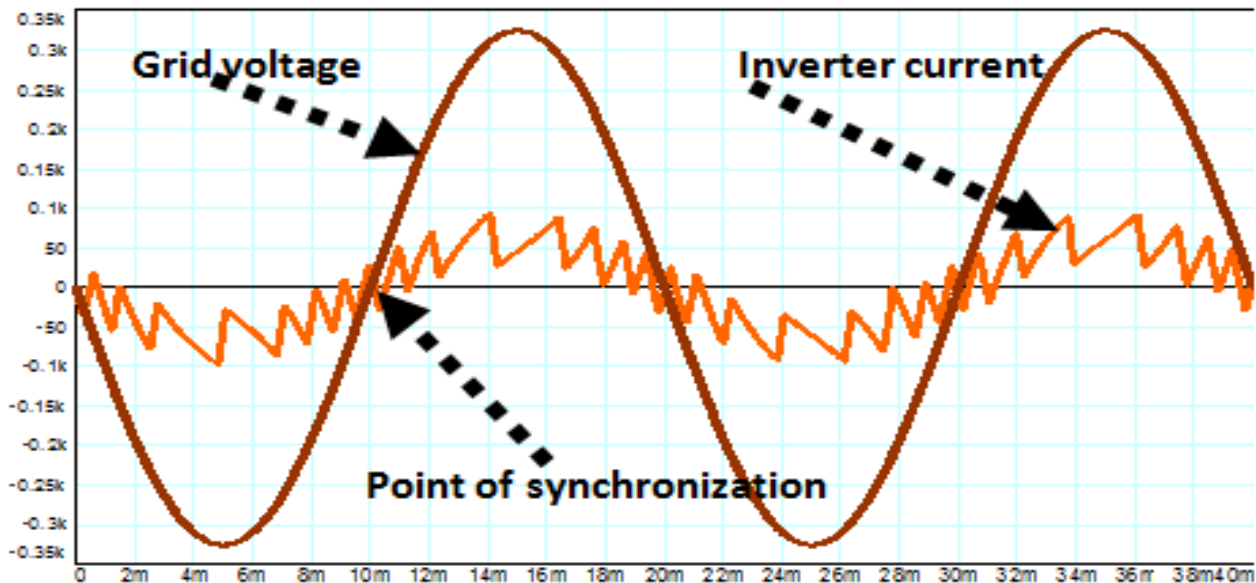


Fig.3: Synchronized waveforms of grid-connected DC-AC converter system under static-band hysteresis current regulator.

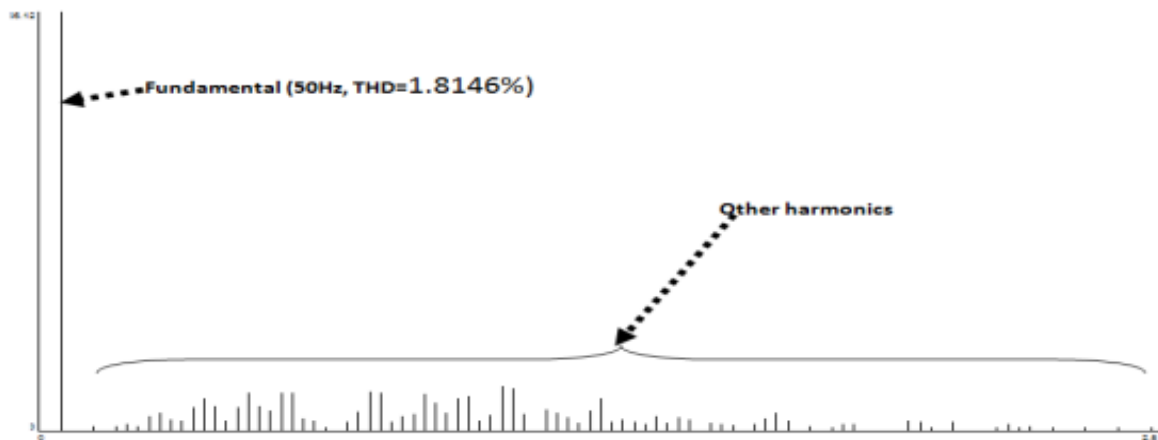


Fig.4: Spectral harmonic content of filtered DC-AC converter output current under static –band current controller.

6. Sine-referenced Current Controller for Harmonization of DC-AC Converter Current and Utility Voltage at Unity Power Factor

The algorithm of the sine-referenced current controller is deduced in eq.7-9 as follow:

$$i_{sref} = I_m \cos(\omega t - \pi/2) \quad (7)$$

The top band limit of the wave shape, is expressed as in eq. 8.

$$i_{sref} = (I_m + h) \cos(\omega t - \pi/2) \quad (8)$$

For the lower band of waveform is

$$i_{sref} = (I_m - h) \cos(\omega t - \pi/2) \quad (9)$$

So, in positive half cycle, i.e. when the reference current is more than zero:

For, $i_{sref}(t) > 0.0$;

If $i_L > i_{up}$; switch OFF MS1 and MS2; switch ON MS3 and MS4; $v_{inv} = -V_{mpp}$

If $i_L < i_{Low}$; switch OFF MS3 and MS4 ; SWITCH ON MS1 and MS2; $v_{inv} = +V_{mpp}$

For negative half part, i.e. when the i_{sref} is below zero.

If $i_{sref}(t) < 0.0$,

If $i_L < i_{up}$; switch ON MS1 and MS2; switch OFF MS3 and MS4; $v_{inv} = +V_{mpp}$

If $i_L > i_{Low}$; switch ON S3 and S4 ; switch OFF S1 and S2;
 $v_{inv} = -V_{mpp}$

If sine-referenced current more than zero and the output inductor current is more than top current band limit, the comparing device sends error current signals to activate turning OFF MS1 and MS2 ; on the other hand turn ON MS3 and MS4. The action ensured current gradient minimization thus compelling the output inductor current to follow sine-referenced current. In addition, the DC-AC converter output voltage is dropped down to be equal $-V_{mpp}$. During the positive half cycle, once the output inductor current is lower than the minor current band limit, the comparing device issues out error current signal to switch OFF MS3 and MS4; and turn ON MS1 and MS2. This instantly pulls up the voltage across the DC-AC converter to be equivalent to $+V_{mpp}$ and also makes the filtered DC-AC converter current to trace and track the sine-referenced current. On the negative half cycle, i.e. when the sine-referenced current is smaller than zero, there exists swapping of the minor current band limit with the top current band bound. Once the output inductor current is smaller than the top current band bound, the comparing device matches the two signals and delivers the error signal that instantly switches ON MS1 and MS2; and turns OFF MS3 and MS4. Therefore, voltage across DC-AC converter equal to $+V_{mpp}$ as well as compelling the output inductor current to be suitably tracing sine-referenced current whereas injecting the output current of the inverter into the grid utility. However, once the output inductor is more than the lower current band bound, then the error current signal sets ON MS3 and MS4; and turns OFF MS1 and MS2. The DC-AC converter voltage becomes the equivalent as boosted voltage due to decrease in current gradient. The uninterrupted transition of voltage caused by spontaneously switching ON and OFF of the power switches as a results the error current signal from the comparator section ensured seamless harmonization of the filtered DC-AC converter current and grid voltage at unity power factor. Hence, the DC-AC converter current harmonic distortion is curtailed to the lowest level. The wave shapes of the sine-referenced current controller and the resultant harmonization of output inductor current and grid voltage were displayed in Fig. 5 and 6.

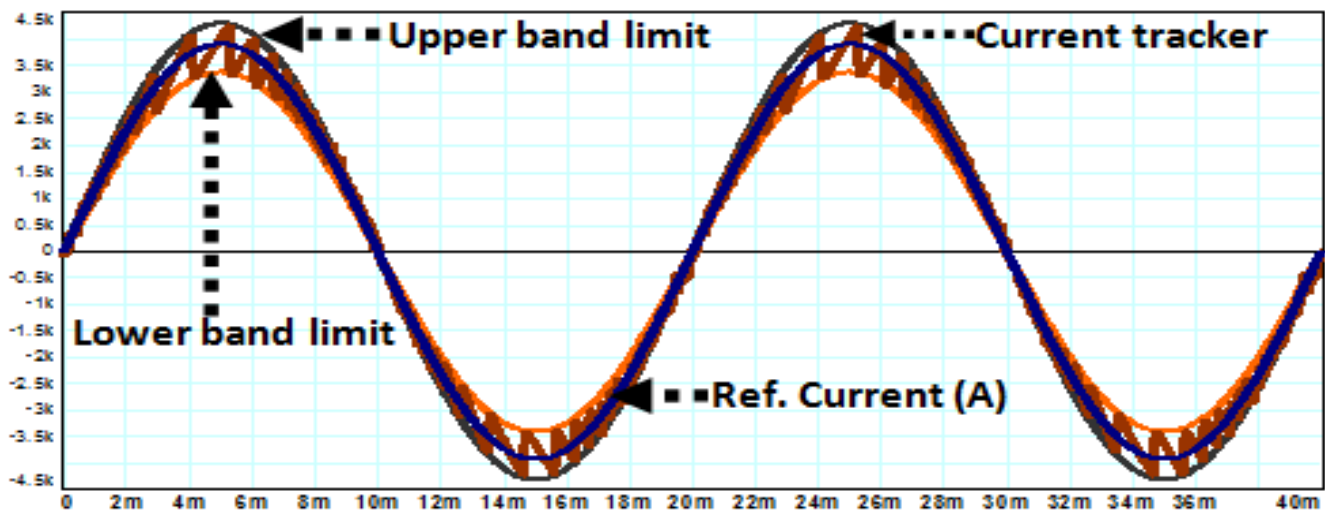


Fig.5 the sine-referenced current controller waveforms

Fig.6 showed a seamless harmonization of filtered DC-AC converter current and grid voltage on the course of power injection into the grid utility under the influence of sine-referenced current controller. This implies that they have the identical frequency and are in the same phase. Furthermore, it means that they began at the same zero angles, reach lowest

point at $\frac{\pi}{2}$ nevertheless of various peaks, meet at zero axes at π for half cycle; and complete the cycle in the same trend at 2π .

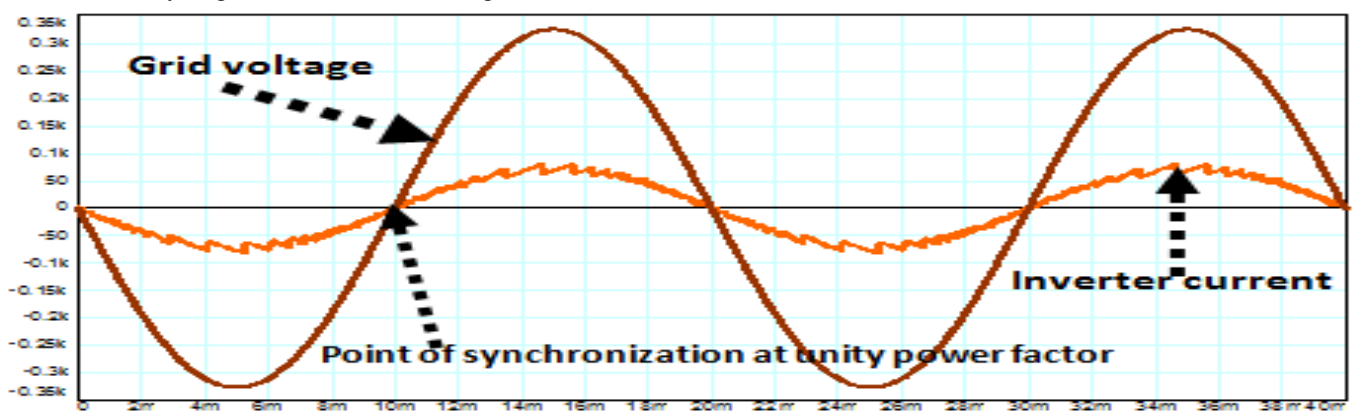


Fig.6: Synchronized inverter current and grid voltage at under sine-referenced hysteresis current controller.

The spectral total harmonic distortion of the sine-reference current controller is shown in Fig.7

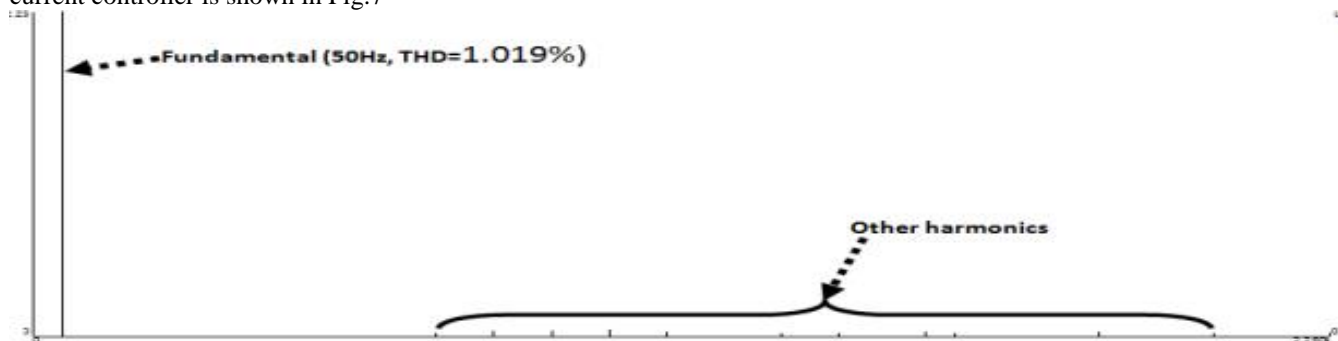


Fig.7: Spectral Harmonic content of filtered DC-AC converter output current under sine-referenced current controller

7. Discussion of Computer Simulated

Results

The simulated results of grid connected DC-AC converter system operated at switching frequency of 23 kHz regulated by sine-referenced and static-band hysteresis of current controllers were carried out in Simplorer software. The sine-referenced current controller illustrated a better performance characteristic than the static-band current controller. It has smaller percentage THD of 1.0195% in Fig 7. The toothed-like waveform of coupling inductor current of static-band current controller is larger than that of sine-referenced current band. The cleaned DC-AC converter current injected into the grid utility under static-band approach in Fig.4 is 99.10A while the current going into the grid utility under the sine-referenced-band approach of Fig.7 is 75.12A. The spectral harmonic spectrum display of the static-band current controller is displayed in Fig.4 of high amplitudes more than that of Fig.7.

Table2. Comparative Results of the two methods

Grid Injecting current controlled method	sine-referenced band current controller	Static -band current controller
Magnitude of injected current	99.10A	75.12A
Band limit range	50 - 130	340 - 430
Total Harmonic Distortion,THD	1.815%	1.019%
Power factor	1.00	0.97
THD	1.815%	1.019%

8. Conclusion

An assessment of total harmonic effects on grid-connected powered inverter using sine-referenced and static-band hysteresis of current controllers has been presented, analyzed and simulated in Simplorer software. From the Table 2, it is observed that the sine-referenced current controlled method offered lower total harmonics distortions, and higher power factor than the static-band current controller. And because of it, there are higher power losses in static-band current controlled scheme than the second one. Moreover, the static-

band current method draws more current from the inverter than the sine-referenced current controller. In other word, it stresses inverter more than other method.

References

- [1] D. A. Paice, *Power Electronic Converter Harmonics: Multi-pulse Methods for Clean Power*, IEEE Press, Piscataway, NJ, 1996.
- [2] B. R. Gupta and C. Singhal, *Power Electronics*, S.K kataria and Sons, 6t edition New Delhi, 2006.
- [3] L.Malesani and D. Divan, *A synchronized resonant link Inverters*, in IEEE, IPEC, pp.1037-1044 2004.
- [4] Hassaine, E.Olias, M.Haddidi and A.Malek, Asymmetric SPWM used in inverter grid Connected, *Revue Des Energies Renouis velables* vol.10 ,No3 pp421-429, (2007).
- [5]. L.Malesani and D.M Divian, *A Synchronized resonant dc link converter for soft-switched PWM*, in IEEE Ann. conf. Rec. , pp 1037-1044, 1989.
- [6]. A.Tripathi, P.C Sen, Comparative analysis of Fixed and sinusoidal hysteresis current Controllerfor voltage source inverters, *IEEE Trans.on Industrial Electronics*, Feb-1992, Vol.39, No.1, pp.63-73.
- [7] C.U. Eya, C.I. Odeh, D.B.N. Nnadi, M.U. Agu, S.E. Obe, Utility Interfaced Pulse-Width Modulation of Solar Fed Voltage Source Inverter Using Fixed-Band Hysteresis Current Controller Method, *Nigerian Journal of Technology (NIJOTECH)*, Vol. 31, No. 1, 2012, pp. 48-57.
- [8] Muhammad H. Rashid, *Power Electronics-Circuits, Devices, and Applications*, 3rd Edition, Dorling Kindersley (India) Pvt.Ltd.2006
- [9] N.Mohan, T.M undeland and W.P Robbins,*Power Electronics-Converters Applications andDesign*, 2nd; John Wiley & Sons, Inc.1995.
- [10] Candidus U. Eya, "Practical implementation of an improved standby boost uninterruptible power supply," *International Journal of Energy and Power Engineering*, pp.1-7, 2014.
- [11] M. Forouzesh, Y. Siwakoti, Saman A. Gorji, F. Blaabjerg, and B. Lehman. Step-Up DC-DC Converters: A Comprehensive Review of Voltage-Boosting Techniques, Topologies, and Applications, *IEEE Transactions on Power Electronics*, vol. 32, no. 12, pp. 9143-9178, 2017
- [12] T. M. Aiswarya and M. Prabhakar, *An efficient High Gain DC-DC Converter for Automotive Applications*, *International Journal of Power Electronics*, vol. 6, pp. 242-252, 2015.
- [13] B. E. Elnaghi, M. E. Dessouki, M. N. Abd-Alwahab and E. Eikholy, *Development of two stage Converter for single-phase Inverter without Transformer for PV systems*, vol. 9, pp. 101-111, 2019.
- [14] Candidus U. Eya , Ayodeji Olalekan Salau and Stephen Ejiolor Oti, *High Performance DC-to-AC Converter Using Snubberless H-Bridge Power Switches and an Improved DC-to-DC Converter*, *International Journal Of Circuits, Systems And Signal Processing*, pp.315-333 Volume 15, 2021. DOI: 10.46300/9106.20

[16] F. Gao, D. Li, P. C. Loh, Y. Tang, and P. Wang, *Indirect dc link voltage control of two stage single phase PV Inverter*, Energy conversion Congress and Exposition, pp. 1166-1172, 2009.

[17] F. He, Z. Zhao, L. Yaun and S. Lu, *A DC-link voltage control scheme for single phase grid-connected PV Inverters* Energy conversion Congress and Exposition, pp. 3941-3945, 2011.

Contribution of Individual Authors to the Creation of a Scientific Article (Ghostwriting Policy)

The authors equally contributed in the present research, at all stages from the formulation of the problem to the final findings and solution.

Sources of Funding for Research Presented in a Scientific Article or Scientific Article Itself

No funding was received for conducting this study.

Conflict of Interest

The authors have no conflicts of interest to declare that are relevant to the content of this article.

Creative Commons Attribution License 4.0 (Attribution 4.0 International, CC BY 4.0)

This article is published under the terms of the Creative Commons Attribution License 4.0

<https://creativecommons.org/licenses/by/4.0/deed.en>